Cite this: DOI: 10.1039/c0xx00000x

www.rsc.org/xxxxxx

ARTICLE TYPE

Halofuginone electrochemical sensor based on molecularly imprinted polypyrrole coated glassy carbon electrode

Abd-Elgawad Radi*, Ismael Abd-Elaziz
Department of Chemistry, Faculty of Science, Dumyat University, 34517 Dumyat, Egypt

Received (in XXX, XXX) Xth XXXXXXXXX 20XX, Accepted Xth XXXXXXXXX 20XX
DOI: 10.1039/b000000x

In this work, a novel and selective polypyrrole (PPy) electropolymerized molecularly imprinted electrochemical sensor (PPy-MIP) for halofuginone (HFG) determination was developed. The imprinted film was fabricated by electropolymerization of pyrrole (Py) in the presence of halofuginone (HFG) onto a glassy carbon electrode (GCE) surface. The electrochemical sensor exhibits a remarkable sensitivity, which might be due to the plenty of cavities for binding HFG through π–π stacking between aromatic rings and hydrogen bonds between nitrogen and oxygen-containing groups of HFG and the PPy. The cyclic voltammetry (CV) and electrochemical impedance spectroscopy (EIS) were employed to characterize the constructed sensor. The effects of pH, the monomer concentration, the number of cycles for the electropolymerization, and the scan rate for the sensor preparation were optimized. Under the optimal conditions, the DPV peak current was linear to the HFG concentration in the range from 7.5×10^{-9} to 1.0×10^{-5} M, with a detection limit of 2.5×10^{-9} M. The prepared sensor also showed acceptable storage stability, reproducibility and regeneration capacity. The electrochemical sensor was applied to determine HFG in chicken meat samples with satisfactory results.

Cite this: DOI: 10.1039/c0xx00000x
www.rsc.org/xxxxxx

ARTICLE TYPE

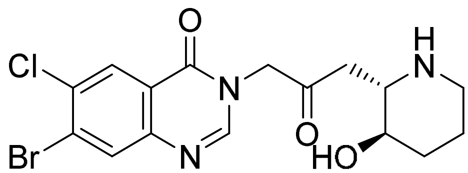

Scheme 1 chemical structure of HFG

Introduction

In poultry, coccidiosis may lead to poor weight gain and reduced egg production [1]. Halofuginone (HFG, (dl-trans-7 bromo-6-chloro-3-[3-(hydroxy-2-piperidyl)acetonyl]-4(3H)-quinazolinone hydrobromide; Scheme 1) is used world-wide to prevent coccidiosis in commercial poultry production [2]. The widespread use of coccidiostats in food producing animals may result a potential exists of coccidiostat residues in the human food chain. Surveillance schemes are in place in most countries to monitor the occurrence of residues in food of animal origin. The concentration of a residue in food is dependent on a number of factors such as dose, excretion, metabolism, absorption and distribution of the drug [3]. The European Agency for the Evaluation of Medicinal Products (EMEA) has set a MRL (Maximum Residue Limit) of 10 and 30 μg kg^{-1} for bovine muscle and liver, respectively[4]. However, no MRL has yet been established by EMEA for HFG residues in poultry. HFG is not licensed in eggs for human consumption. It should be free from HFG residues. However, several works have shown that HFG can potentially be transferred to eggs [5].

To date, a range of analytical techniques has been applied for HFG determination in different samples, including GC and HPLC [6-10]. Immunoassay techniques for the determination of HFG in chicken plasma [11] and tissue [12] have also been described. All of these methods use HPLC with UV detection and have been described for both chicken tissues[13] and eggs[14]. Most of these methods suffered, expensive analysis settings, labor-intensive sample preparation or interferences. Hence, an alternative method with high selectivity and sensitivity would be essential in rapid determination of HFG in food stuff samples.

Electrochemical methods have been proved to be excellent alternatives in the analytical chemistry field due to their simplicity, low cost, short analysis times and high sensitivity. To the best of our knowledge, there are no previous reports on the electrochemical oxidation of HFG. The MIPs have been widely used as recognition elements for the development of electrochemical sensors [15-18], which were formed on the electrode surface by an electropoly-merization technique. Electropolymerization allows for the generation of a rigid, uniform, and compact MIP film with good adherence onto an electrode surface of any shape and size [19, 20]. Moreover, the thickness and density of the film is adjustable by controlling polymerization conditions. Therefore, many MIP-based sensors have been prepared and used to recognize and detect different molecules in preference to other closely-related compounds [17, 21]. With their intrinsic properties of selectivity, the application of MIPs in electrochemistry is intriguing to improve the response of the electrode to target molecules.

With regard to the selection of the polymer materials, polypyrrole has been one of the most extensively studied materials during the last decade because it can be used in a neutral pH region and its stable film can be deposited easily, chemically and electrochemically onto a variety of substrate materials and good biocompatibilitystability in ambient conditions and thickness controllability [22].

In the present study, a novel MIP-based electrochemical sensor was fabricated successively by electropolymerizing pyrrole in the presence of HFG onto a GCE surface. The prepared sensor was characterized by cyclic voltammetry (CV), and electrochemical impedance spectroscopy (EIS). Under the optimized conditions, the sensor exhibited good adsorption and a high recognition capacity for HFG. The prepared PPy-GCE-MIP exhibit significant sensitivity and selectivity in the electrochemical detection of HFG in real samples.

Experimental

Materials

The standard halofuginone hydrobromide sample supplied from Roussel, was used without further purification. Pyrrole was purchased from Fluka (Fluka Chemie AG, Switzerland). All other reagents were of analytical-reagent grade, and double-distilled deionized water was used for all solutions. Stock solution (1.0×10^{-2}M) HFG was prepared in methanol and stored in a refrigerator at 4°C. Standard solutions were prepared daily by diluting of the stock solution with the selected supporting electrolyte. Orthophosphoric acid 85%, potassium dihydrogen phosphate KH_2PO_4, disodium hydrogen phosphate Na_2HPO_4, and sodium phosphate Na_3PO_4 were mixed with different amounts and diluted with distilled water to obtain the phosphate buffer solutions (0.02 M) with the required pH.

Apparatus

Electrochemical measurements were performed with AU-TOLAB PGSTAT 302N potentiostat with FRA module for electrochemical impedance (EIS) measurements (Metrohm Autolab b.v., the Netherlands), using NOVA software. A three-electrode system was composed of a glassy carbon (BAS model MF-2012, Φ= 3 mm) working electrode, an Ag/AgCl/3M KCl (BAS model MF-2063) reference electrode and a platinum wire (BAS model MW-1032) counter electrode. All pH-metric measurements were made on a CG 808 (Schott Gerate, Germany) digital pH-meter with glass combination electrode, which was previously standardized with buffers of known pHs.

Procedure

Preparation of polymer-coated electrodes

The surface of GCE was polished with aqueous alumina slurries on a metallographic polishing cloth, with successive decrease in particle size and the remaining particles on the surface were removed by ultrasonic treatment in Mili-Q water. Then the electrode was oxidised from 0.0 to 1.4 V vs. Ag/AgCl. The GCE was immersed into $NaClO_4$ solution containing pyrrole and HFG. Next, cyclic voltammetry (CV) was performed several cycles, obtaining the polymer-modified GCE. Subsequently, the embedded HFG were extracted by scanning between -0.6 and +1.3 V in 0.02 M phosphate buffer solution (PBS, pH 7.0) for several cycles until no obvious oxidation peak for HFG could be observed; this process gave MIP-modified GCE (GCE-MIP). As a control a non-molecularly imprinted polymer-(NIP)-modified GCE-NIP was also prepared and treated in exactly the same manner, except HFG in the electropolymerization process was excluded.

The current–potential curves were recorded using either CV or differential pulse voltammetry (DPV). The following parameters were used throughout unless otherwise stated: cyclic voltammetry, scan rate 100 mV s and operating conditions for the DPV were: pulse amplitude, 50 mV; pulse width, 50 ms; scan rate, 20 mVs−1. Electrochemical impedance measurements were performed in the presence of equimolar concentrations, $K_3[Fe(CN)_6]/K_4[Fe(CN)_6]$ 1.0 mM as redox probe at the formal redox potential, using a sinusoidal ac potential perturbation of 5 mV, in the frequency range 100 kHz to 500 mHz, and readings were taken at 20 discrete frequencies per decade. The impedance spectra were plotted in the form of Nyquist plots.

Results and discussion

Electrochemical behaviour of HFG

There were no previous electrochemical data available concerning the redox behaviour of HFG. CV is often the first experiment performed in an electroanalytical study. In particular, it offers a rapid location of redox potentials of the electroactive species, and convenient evaluation of the effect of media upon the redox process. Therefore, HFG was subjected to a preliminary CV experiments for 5.0 $\times 10^{-5}$ M HFG in phosphate buffer background solutions over the pH range 3.0–10.0 on the GCE with the aim to characterize in detail its electrochemical redox behaviour. Fig. 1 shows representative CV obtained at GCE. HFG is oxidized, yielding one oxidation peak.The oxidation process involved is irreversible, as no cathodic peak was found at scan rates between 10 and 100 mVs^{-1}. A positive shift in the peak potential was observed with increasing sweep rate, which confirms the irreversible nature of the oxidation process. The relationship between the oxidation peak potentials and scan rates can be described as following: $E_{pa} = 0.0542 \log \upsilon + 0.9107$, r = 0.9949. According to Laviron’s theory [23], the slope was equal to 2.303RT/αnF. Then the value of $\alpha\, n_a$ was calculated as 0.56. As for a totally irreversible electrode reaction process, α was assumed as 0.5. On the basis of the above discussion, the n_a was calculated to be 1.0 which indicated that one electron was involved in the oxidation process of HFG at the GCE electrode.

The diffusion control of the processes was evident from the linear relationship between current and the square root of the scan rate. This evidence is confirmed by plotting the logarithm of peak current (log i_{pa}) versus the logarithm of the scan rate (log ν). The plots yielded a straight lines with slopes close to the theoretical value of 0.50, which is expected for an ideal reaction condition for diffusion-controlled electrode process[24].

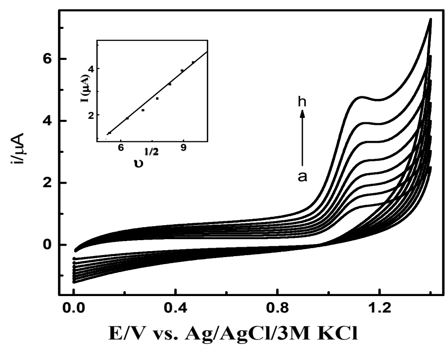

Fig. 1:CVs obtained for 5.0× 10^{-5}M HFG at GCE in 0.2 M PBS pH 9.0 at ν=20 (a), 30 (b), 40 (c), 50 (d), 60(e), 70 (f), 80 (g) and 90(h) mV s^{-1}.Inset: i_P-ν $^{1/2}$plot

DPV was also used to investigate the effect of pH on the electrochemical oxidation of 5.0 $\times 10^{-5}$M HFG in aqueous supporting electrolytes over a pH range from 3.0 to 10.0 (Fig. 2) as already found by CV. The peak potential of anodic peak of HFG is shifted linearly towards more negative values and peak current also increased up to pH = 7.0 and afterwards decreased with increasing pH values. The relation between the peak potential (E_{pa}) and the solution pH is linear in the pH range studied (Fig. 3b). The slope = -100.0 (mV per pH) = (60/α) × (m/n) (α: transfer coefficient. m and n: number of proton and electrons involved in the reaction. respectively). The slope show that one protons take part in the rate-determining step [25]. A plausible mechanism may involve the electrochemical oxidation of the nitrogenous group of the 4-quinazolinone moiety [26]. The oxidation of HFG occurs with a transfer of one electron and one proton.

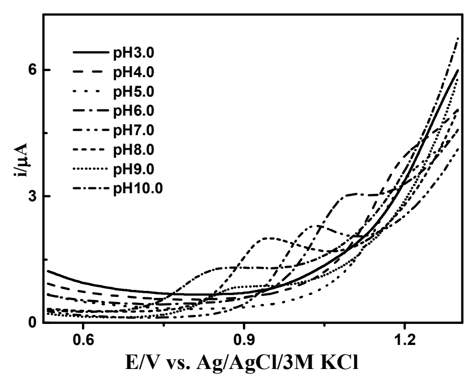

Fig. 2: Effect of pH on determination of 1.0 × 10^{-5} M HFG using DPVs at GCE in 0.2 M phosphate buffer solution.

Electropolymerization of Py

Figure 3 shows the CVs recorded during the electropolym-erization of Py in 0.1 mol/L pyrrole + 1.0 mol/ $NaClO_4$ aqueous solution on the GCE electrode. The pair of broad oxidation and reduction waves centered at ∼0.25 V is the PPy redox wave.The voltammetric response decreased with the voltammetric cycle number. It suggests that a compact and insulating film is formed and coated onto the GCE surface progressively, leading to the reduction of the voltammetric response. An anodic peak appeared at the higher potential of 1.00 V in the first anodic potential scan (Fig.3 curve), corresponding to the oxidation of HFG. This oxidation peak indicates that the template is becoming part of the polymeric chain. HFG molecules diffuse towards the surface of the GCE during the electropolymerization process and trapped into the polymer matrix. The creation of the molecular imprints is favored by the diffusion of the electroactive template, generating a far higher number of recognition sites during the electrodeposition of the polymer. The HFG template molecules are trapped in the polymer matrix as a result of the ability of these molecules to interact with the Py units.

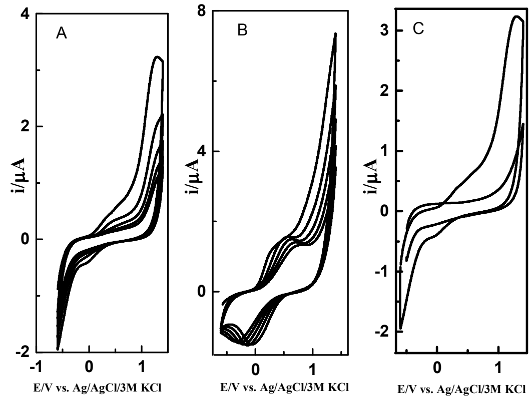

Fig.3: CVs taken during the electropolymerization of 0.01 M pyrrole in 0.1 M $NaClO_4$ supporting electrolyte in the presence of (A) 0.0 and (B) 2.5 mM HFG at GCE. (C) CV curve of blank sample on an MIP film after extraction of HFG; scan rate: 100 mV s^{-1}.

One can reasonably speculate a formation of hydrogen bonds between nitrogen and oxygen-containing groups of HFG and the PPy with a specific spatial distribution, which maximizes the attractive interactions between the recognition sites and the template. These favorable interactions and complementary cavities create the microenvironment for recognition of HFG molecules. The extraction of HFG molecules was completed by cycling between -0.6 and 1.3 V in 0.02 M phosphate buffer pH 7.0, until all HFG molecules were stripped from the imprinted PPy film and the oxidation peak corresponding to HFG was no longer observed (Fig.3 curve c1). The obtained differential pulse voltammograms for 1×10^{-5} M HFG at the PPy-GCE-MIP, PPy-GCE-NIP and bare GCE electrodes are presented in Fig. 4. It was noteworthy that PPy-GCE-MIP (curve a) electrode produced a noticeably higher oxidation peak current at 1.04 V than the bare GCE (curve b) and PPy-GCE-NIP (curve c). The current response of PPy-GCE-MIP was nearly 5.4 times that of bare GCE. It was evident that the PPy-GCE-MIP electrodes adsorbed significant amount of HFG from the sample solution, in comparison with GCE and PPy-GCE-NIP electrodes. This behavior is presumably due to the selective binding sites in the synthetic MIP particles, which are complementary to the HFG in size, shape and functional groups.

Influences of Template Concentration, Buffer, and Cycle Number on Polypyrrole Deposition

The recognition ability could easily be adjusted by controlling the thickness of the molecularly imprinted PPy film. The thickness of the deposit film is proportional to the template concentration, electrolyte concentration and scan number on PPy deposition. The current response increased with Py concentration in the range of 0.005–0.050 M and reached maximum with the concentration of 0.025 M, and then decreased with further increasing the concentration of Py monomer. Thus, 0.025 M Py monomer was chosen to obtain the highest sensitivity for the determination of HFG.

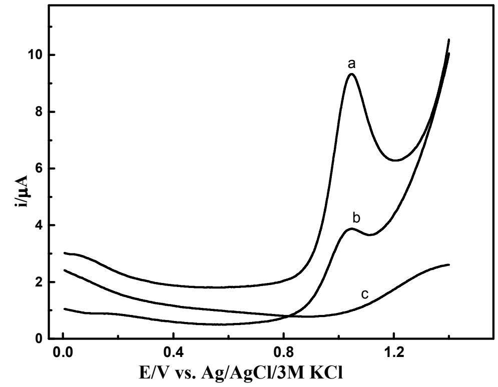

Fig.4: DPVs of 5.0× 10^{-5}M HFG in 0.2 M phosphate buffer solution of pH 9.0 at (a) pPy-GCE-MIP, (b) GCE, and (c) pPy-GCE-NIP electrodes.

The response of the MIP/GCE firstly increased with increasing the number of cycles up to 10, and then decreased considerably above this number of cycles. The MIP/GCE produced at lower number of cycles exhibited less sensitivity, probably due to the small number of recognition sites formed in the polymer matrix. More cycles than needed could lead to more extensive electropolymerization, and consequently, to the formation of thicker sensing film with less accessible imprinted sites. The highest current difference between the GCE-MIP and GCE-NIP for HFG was obtained by applying 10 cycles in the electropolymerization. Therefore, the polymerization cycles was chosen to be 10. The influence of HFG on the polymerization of Py was further studied with different concentrations of HFG between 0.5 and 5.0 mM. As the concentrations of template molecule applied to the polymerization process increases in a range from 50 M to 500 µM, the amount of template entrapped in the matrix also increases until it reaches equilibrium at about µM and the current intensity that corresponds to the oxidation of the entrapped template tends to become stable as no further quantity of template can be incorporated into the polymeric chain. The concentration of $NaClO_4$ supporting electrolyte was an important parameter for MIP fabrication. Its influence was investigated over the range from 0.01 M to 0.50 M. The best results were obtained employing 0.10 M $NaClO_4$, further increase in the concentration did not improve the analytical signal. All the optimized parameters were then used for further work.

Electrochemical characterization of the imprinted sensor

Cyclic voltammetry (CV) and electrochemical impedance spectroscopy (EIS) were used to characterize the imprinted sensor. The changes of interfacial features of the electrode were probed in the presence of the reversible redox couple, $[Fe(CN)_6]^{3-}/[Fe(CN)_6]^{4-}$. CVs on the bare GCE, GCE-NIP and GCE-MIP are shown in Fig. 5A. A couple of typical redox peaks of couple appear on the bare GCE (curve a). Only a very small background response, however, is observed on GCE-MIP (curve c) or GCE-NIP (curve c) over the potential range, due to the fact that the film coated on the electrode was compact and less conductive than the GCE and there are almost no channels for the active probe to approach the GCE surface. It is also noted that compared with the bare GCE, an obvious current decrease appeared when using the GCE-MIP after the template removal (curve d). This may result from the low conductivity of the film coated on GCE, though the cavity caused by the removal of HFG molecule forms some channels for hexacyanoferrate to arrive at the electrode surface. Curve d shows the same GCE-MIP after being saturated with 0.1 mM HFG, where only a small peak appears due to partial binding sites in MIP film occupied by HFG.

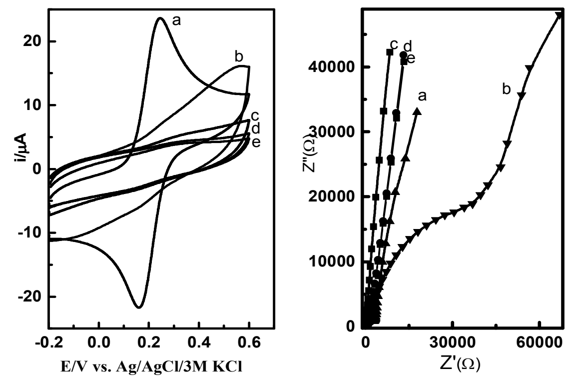

Fig.5:(A) CVs and (B) EIS recorded in a 0.01 M [Fe(CN)6]3−/[Fe(CN)6]4− in phosphate buffer solution of pH 7.0 for bare GCE (a), GCE-MIP before extracting HFG (b), GCE-NIP (c), and GCE-MIP after extracting HFG (d) and GCE-MIP after incubating in 5.0×10^{-5} M HFG solution (e).

Electrochemical impedance spectroscopy (EIS) can provide useful information on the impedance changes of the electrode surface. Fig. 5B illustrates the typical results of EIS (presented in the form of the Nyquist plot) of the bare GCE, GCE-NIP and GCE -MIP, respectively, with $[Fe(CN)_6]^{3-}/[Fe(CN)_6]^{4-}$ as a redox probe. Here, the impedance spectra included semicircle portions at higher frequencies and linear portions at lower frequencies, which corresponded to the electron-transfer resistance and the diffusion process, respectively. As shown in curve a, for the bare GCE there is a small semicircle domain present, implying that there was improved diffusion of ferricyanide toward the electrode surface. With the coating of the polymer, the resultant GCE-MIP (curve b), or GCE-NIPs (curve c) displayed obvious increases in their interfacial resistances, implying that hindered pathways for the electron transfers had formed with the polymer. A non-conducting polymer of oxidized PPy_{ox} , prepared from an aqueous solutions of pyrrole, is formed. The PPy chain is sensitive to the pH of the solution. The chain undergoes a deprotonation process in basic solutions, which causes the transformation of PPy into a non-conducting polymer probably of quinoid structure accompanied by the deintercalation of the original counter anions. In acidic solutions, a PPy chain is protonated. However, the protonation has only a small effect on the electronic structure of the chain, causing only slight increase of the PPy conductivity, of the counter anions and of the excess hydrogen content of the polymer[27]**.** The resistance was practically high for the GCE-MIP film fully loaded with the HFG template (curve d), indicating that the diffusion of the probe was effectively prevented because the imprinted molecular cavities were occupied by the HFG molecules. A significant decrease in R can be observed on the GCE-MIP after removing the template, apparently, because the probe diffusion through the film, populated by vacated imprinted cavities (curve d), was enabled. Furthermore, after immersing the GCE-MIP in 5.0×10^{-5} M HFG, the resistance substantially increased which could be attributed to the rebinding of HFG into the imprinted cavities and to the blocking of the arrival of the probe onto electrode surface (curve e). These results are accordance with CV data as described in detail above.

Optimization of electrochemical measurement conditions

Effect of pH

The pH effect of sample solution at different pH values (3.0–10.0) on the electrochemical response was investigated for HFG with a concentration of 5.0×10^{-5} M at the GCE-MIP electrode. The current signal was increased when the pH values increased from 6.0 to 8.0, and then had no considerable variation from pH 8.0 to 10.0. The effective recognition of target molecules is attributed to not only the complementary interaction between molecules and polymer but also the interplay of hydrophobic effect. When the hydrogen bonding between molecules is weakened by increasing pH, the significance of hydrophobic effect will be more dominant[28]. Therefore, phosphate buffer solution with pH at 7.0 was chosen as a supporting electrolyte for the HFG analysis.

Optimization of adsorption time

The adsorption kinetics of HFG was investigated by varying the adsorption time from 30 s to 10 min, and the initial concentration of HFG kept constant at 5.0×10^{-5} M. The peak current increased rapidly with the incubation time and then leveled off after 2 min, presumably resulting from reaching the absorption balance between the sample solution and surface of MIPs-GCE electrode. The result reveals rapid response equilibrium of HFG molecules to PPy-GCE-MIP, which might be due to the surface binding sites of PPy-GCE-MIP through π–π stacking between aromatic rings and hydrogen bonds between and nitrogen and oxygen-containing groups of the Py units and HFG. Thus, the absorption time of 2 min was selected as an optimum for further experiments.

Analytical performance

The electrochemical behavior and determination of the HFG were investigated using differential pulse voltammetry (DPV) and square-wave voltammetry (SWV) to find the best analytical conditions. After optimizing the experimental parameters for the proposed methods, the analytical curves were constructed by adding small and equal volumes of the concentrated standard solutions of the analyte to the supporting electrolyte to obtain the final concentrations in the range of 7.5×10^{-9}–1.0×10^{-5} M of HFG. Then, electroanalytical procedures were developed for HFG using SWV and DPV. First, optimization of the parameters that affect the response obtained by these voltammetric techniques was performed; the obtained optimum values are: (a) for DPV, Step potential 6 mV, modulation amplitude 50 mV and scan rate 20 mV/s; (b) for SWV, frequency (f) of 50 Hz, amplitude (a) of 50 mV, and scan increment (DEs) of 4 mV. These values were used in the development of the respective electroanalytical procedures for the determination of HFG. The thus obtained analytical curves presented good linearity, as can be seen in Fig. S1 in the ESI.† A linear calibration graphs have been constructed by plotting the corresponding value of voltammetric peak current versus HFG concentration. The linear regression equations were expressed as: I (µA) =0.38082 CHFG (µA)+ 0.00316 and I (µA) =0.98632 CHFG (µA)+ 9.8678×10^{-5}. The LOD at MIPs based electrochemical sensor was evaluated according to the 3Sb/m criteria, where Sb is the standard deviation of the blank and m is the slope of the linear calibration curve [29]. Thus, the obtained LOD values were found to be 2.5 × 10-9 M and 4.5 × 10-9 M for DPV and SWV, respectively. The electroanalytical procedure that couples DPV and an MIP electrode yielded the best values for detection limit. Consequently, DPV was the technique selected for the voltammetric determination of HFG, as presented hereinafter. On the other hand, adequate accuracy and precision values were obtained for the determination of HFG by DPV. The relative standard deviation (RSD) of determination was below 3.7% for 1.0×10^{-6} M HFG with six repeated measurements. Furthermore, no significant change in analytical performance was observed when the electrodes were used 3 assays every day for one week (%RSD ≤ 4.8%).

Reproducibility, repeatability, and storage stability of the MIP sensor

To test the reproducibility of the proposed technique, three MIP sensors were constructed under identical experimental conditions. The current change was obtained for 1.0×10^{-6} M HFG, by using each of the MIP sensors. The relative standard deviation (RSD) was 3.5 %. The repeatability of one electrode was also examined and the calculated RSD was about 4.2 % (n=5). The sensor can retain 90 % of its original response after the electrode was stored for 1 month in air at room temperature, suggesting acceptable storage stability.

Practical application in real samples

In order to evaluate the feasibility of the developed method for real sample analyses, the determination of HFG in chicken meat was carried out using the MIP based electrochemical sensor. Quantification was performed using matrix-matched standards prepared by adding known amounts of the stock solutions to blank sample matrix to obtain concentrations of 10, 20, 50, 100 and 250 µg kg^{-1} in matrix. Firstly, the samples treatment involved protein precipitation. Specifically, 1.0 g chicken meat sample and 1.0 ml of HFG standard solution with different concentrations was added in 1.0 ml water. Then, 3.0 mL of trichloroacetic acid (20%, wt%) solution was added to the mixed solution for protein precipitation. The mixture was vortexed for 1 min, and then centrifuged at 4000 rpm for 10 min. The supernatant was collected and filtered through a 0.22 µm membrane filter. No other pretreatment process was performed. Next, 1.0 mL of the supernatant was diluted 5 times with PBS (pH=7.0), vigorously vortexed for 10 s. and transferred to the electrochemical cell for the recovery determination. DPVs for the determination of HFG in chicken meat at MIP are shown in Fig 6:

The recoveries of the spiked HFG, based on five parallel measurements, are listed in Table 1. The values of recoveries are found to be from 97.40 to 103.25%, and %RSD ranged from 2.7 to 5.3%, indicating that the sensor has good accuracy and great potential for practical application for the analysis of HFG in real samples.. The LOD was found to be 2.5µgkg^{-1}. Comparison of the data as obtained by LC-UV [30] and DPV revealed that the concentrations determined by both methods were equivalent.

In this study some coccidiostats such as dinitrocarbanilide, imidocarb, toltrazuril, clopidol, lasalocid and arprinocid were chosen to evaluate the effect of coexisting substances on the recovery of HFG by the MIP. In this study, binary solutions of constant amount of HFG (10.00 µg kg-1)) and different concentrations of the coexisting substances were prepared and the recoveries of HFG were determined. The tolerance limit was considered as the coexisting concentration making a relative error less than 5% in the recovery of HFG. It is revealed that the coexisting substances have no interfering effect on the recovery of HFG.

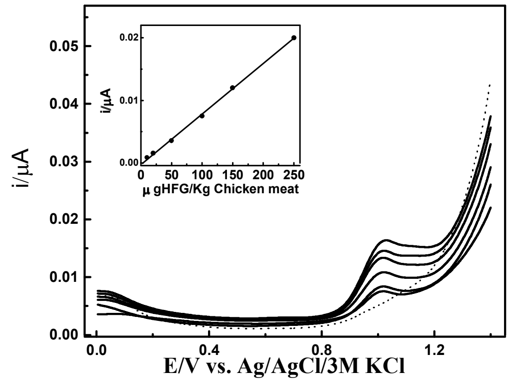

Fig 6: DPVs for the determination of HFG 10.0–250.0 µg per Kg meat (solid lines), from bottom to top, adjusted with 0.2 M phosphate buffer solution of pH 7.0 at MIP; the dotted lines (...) represent the blank; inset: calibration curve of HFG in chicken meat at MIP. Step potential 6 mV, modulation amplitude 50 mV and scan rate 20 mV/s.

Conclusion

In conclusion, PPy-GCE-MIP has been fabricated via a facile process. The unique PPy with plenty of cavities could bind HFG through π–π stacking between aromatic rings and hydrogen bonds between nitrogen and oxygen-containing groups of the polymer and HFG. Such electrochemical sensor exhibits a high current response, low detection limit and good selectivity. Moreover, the developed method offers a promising advance for detecting HFG in foodstuff samples and showed high resistances against the interference effects of various potential interferents in chicken meat.

Table 1. Recovery tests of HFG in chicken plasma and liver samples.

Added (µg kg^{-1})	Found (µg kg^{-1})	Recovery(%	RSD[a] (%)
10.00	9.74	97.40	2.7
20.00	20.66	103.30	2.5
50.00	51.07	102.13	3.1
100.00	103.25	103.25	4.2
250.00	256.10	102.44	5.3

[a]RSD value reported is for n=5.

References

1. P. L. Long, *Coccidiosis of man and domestic animals*, CRC Press Inc., 1990.
2. M. J. Kennedy, *Coccidiosis in chickens*, Alberta Agriculture, Food and Rural Development, 2001.
3. J. E. Roybal, A. P. Pfenning, S. B. Turnipseed and S. A. Gonzales, *Analytica chimica acta*, 2003, **483**, 147-152.

4. S. Yakkundi, A. Cannavan, P. Young, C. Elliott and D. Kennedy, *Analytica Chimica Acta*, 2002, **473**, 177-182.
5. P. Long, K. SHERIDAN and L. McDougald, *Poultry science*, 1981, **60**, 2342-2345.
6. A. Anderson, D. H. Christopher and R. N. Woodhouse, *Journal of Chromatography A*, 1979, **168**, 471-480.
7. A. M. Committee, *Analyst*, 1983, **108**, 1252-1256.
8. C. Tillier, E. Cagniant and P. Devaux, *Journal of Chromatography A*, 1988, **441**, 406-416.
9. L. Křivánková, F. Foret and P. Boček, *Journal of Chromatography A*, 1991, **545**, 307-313.
10. A. Anderson, E. Goodall, G. W. Bliss and R. N. Woodhouse, *Journal of Chromatography A*, 1981, **212**, 347-355.
11. L. Clarke, T. L. Fodey, S. R. Crooks, M. Moloney, J. O'Mahony, P. Delahaut, R. O'Kennedy and M. Danaher, *Meat science*, 2014, **97**, 358-374.
12. V. Hagren, S. R. Crooks, C. T. Elliott, T. Lövgren and M. Tuomola, *Journal of agricultural and food chemistry*, 2004, **52**, 2429-2433.
13. R. C. Beier, T. J. Dutko, S. A. Buckley, M. T. Muldoon, C. K. Holtzapple and L. H. Stanker, *Journal of Agricultural and Food Chemistry*, 1998, **46**, 1049-1054.
14. S. Yakkundi, A. Cannavan, C. Elliott, T. Lövgren and D. Kennedy, *Journal of Chromatography B*, 2003, **788**, 29-36.
15. T. Alizadeh, M. Zare, M. R. Ganjali, P. Norouzi and B. Tavana, *Biosensors and Bioelectronics*, 2010, **25**, 1166-1172.
16. Q. Yang, Q. Sun, T. Zhou, G. Shi and L. Jin, *Journal of agricultural and food chemistry*, 2009, **57**, 6558-6563.
17. X. Kan, H. Zhou, C. Li, A. Zhu, Z. Xing and Z. Zhao, *Electrochimica Acta*, 2012, **63**, 69-75.
18. B. B. Prasad, R. Madhuri, M. P. Tiwari and P. S. Sharma, *Biosensors and Bioelectronics*, 2010, **25**, 2140-2148.
19. A. Gómez-Caballero, N. Unceta, M. Aranzazu Goicolea and R. J. Barrio, *Sensors and Actuators B: Chemical*, 2008, **130**, 713-722.
20. C. Pellicer, A. Gomez-Caballero, N. Unceta, M. A. Goicolea and R. J. Barrio, *Analytical Methods*, 2010, **2**, 1280-1285.
21. X. Kan, T. Liu, H. Zhou, C. Li and B. Fang, *Microchimica Acta*, 2010, **171**, 423-429.
22. A. Ramanavičius, A. Ramanavičienė and A. Malinauskas, *Electrochimica Acta*, 2006, **51**, 6025-6037.
23. E. Laviron, *Journal of Electroanalytical Chemistry and Interfacial Electrochemistry*, 1974, **52**, 355-393.
24. E. Laviron, *Journal of Electroanalytical Chemistry and Interfacial Electrochemistry*, 1979, **101**, 19-28.
25. P. Zuman, *Journal of Solid State Electrochemistry*, 2006, **10**, 841-851.
26. S. C. Pakrashi, S. Chattopadhyay and A. K. Chakravarty, *The Journal of Organic Chemistry*, 1976, **41**, 2108-2111.
27. Q. Pei and R. Qian, *Synthetic metals*, 1991, **45**, 35-48.
28. X.-J. Wang, Z.-L. Xu, J.-L. Feng, N.-C. Bing and Z.-G. Yang, *Journal of Membrane Science*, 2008, **313**, 97-105.
29. J. N. Miller and J. C. Miller, *Statistics and chemometrics for analytical chemistry*, Pearson Education, 2010.
30. P. P. J. Mulder, P. Balzer-Rutgers, E. M. te Brinke, Y. J. C. Bolck, B. J. A. Berendsen, H. Gerçek, B. Schat and J. A. van Rhijn, *Analytica Chimica Acta*, 2005, **529**, 331-337.